

Theoretical Methods for Giant Resonances

Gianluca Colò

Abstract The Random Phase Approximation (RPA) and its variations and extensions are, without any doubt, the most widely used tools to describe Giant Resonances within a microscopic theory. In this chapter, we will start by discussing how RPA comes out naturally, if one seeks a state with a harmonic time dependence in the space of one particle-one hole excitations on top of the ground state. It will be also shown that RPA is the simplest approach in which a “collective” state emerges. These are basic arguments that appear in other textbooks but are also unavoidable as a starting point for further discussions. In the rest of the chapter we will give emphasis to developments that have taken place in the last decades: alternatives to RPA like the Finite Amplitude Method (FAM), state-of-the-art calculations with well-established Energy Density Functionals (EDFs), and progress in *ab initio* calculations. We will discuss extensions of RPA using as a red thread the various enlargements of the one particle-one hole model space. The importance of the continuum, and the exclusive observables like the decay products of Giant Resonances, will be also touched upon.

Introduction

Giant resonances are among the strong evidences of the fact that nuclei display highly collective motion. Collective rotations are also among these evidences but they take place on a slower timescale. Cluster radioactivity, or spontaneous and induced fission, are even slower phenomena: they go often under the name of “large amplitude” phenomena as the nucleus undergoes large fluctuations and changes in its configuration (Nakatsukasa et al. (2016)). On the other hand, Giant Resonances are “small amplitude” phenomena, namely small oscillations around the ground-

Gianluca Colò

Dipartimento di Fisica, Università degli Studi di Milano, and INFN, Sezione di Milano, Via Celoria 16, 20133 Milano (Italy), e-mail: gianluca.colò@mi.infn.it

state configuration that are, to a first approximation, amenable to a harmonic description. Thus, we note in passing the remarkable fact that coherent behaviours of many, if not all, nucleons display at different energy scales.

Giant resonances are prominent peaks that show up in the nuclear response around $\approx 10\text{-}30$ MeV. ‘‘Response’’ is here a generic wording that may refer to various external fields. If we consider a generic inelastic reaction, we can safely state that giant resonances have a cross section which is larger than those associated with the other states. We shall use the notation F for a generic external field and use the standard definition of strength function $S(E)$ associated with this field, that is

$$S(E) = \sum_n |\langle n|F|0\rangle|^2 \delta(E - E_n), \quad (1)$$

where $|0\rangle$ and $|n\rangle$ are the ground state and excited states, respectively. E_n is the excitation energy of the state $|n\rangle$.

Eq. (1) refers to discrete states but in the case at hand we are above the separation energy and clearly in the continuum part of the nuclear spectrum. The equation can be easily generalised to the case in which the states have an intrinsic width Γ_n , e.g., in the form

$$S(E) = \sum_n |\langle n|F|0\rangle|^2 \frac{\Gamma_n}{(E - E_n)^2 + \frac{\Gamma_n^2}{4}}. \quad (2)$$

Indeed, in this chapter, we do refer to states that have clearly the shape of a resonance, i.e. are characterised by a peak energy E and a conspicuous width Γ , and definitely emerge on top of the background of the other excited states.

This chapter is related to theoretical methods and in essentially all of them one calculates the whole spectrum associated with states having given quantum numbers J^π (total angular momentum and parity). Situations in which the prominent states emerge much less with respect to the background, in which the states are many and the widths are large so that resonances do overlap, or even in which no collective behaviour shows up, may be found. In other words, giant resonances may or may not show up in the response associated with a given J^π , and the physical information they carry may be very relevant or not.

Often, one carries out studies of Giant Resonances either in order to test the nuclear Hamiltonian and extract information like the associated Equation of State (EoS), or to see if the theoretical method that is employed captures all the relevant many-body correlations. The two aspects are not fully disconnected, though. To give only one example here, the simplest nuclear Giant Resonance is the Isoscalar Giant Monopole Resonance or ISGMR (Blaizot (1980); Garg and Colò (2018)). We shall provide in the next pages a classification of Giant Resonances, and their names will be fully clarified. Here, let us just say that the ISGMR is also called the ‘‘breathing mode’’ as it is a mode in which the nucleus shrinks and expands. Intuitively, it must be related with the nuclear compressibility. In other words, a nuclear Hamiltonian, which is able to reproduce the properties of the ISGMR, should also be able to reproduce the correct value of the nuclear matter compressibility (taking care of experimental and theoretical uncertainties). Obviously, this argument holds if there

are good reasons to believe that the correlation between ISGMR energy and nuclear incompressibility is obtained in a sound many-body method.

From the historical viewpoint, the first evidence of a giant resonance has been found in the response of the nucleus to real photons (Berman and Fultz (1975)). A large resonance has been found systematically in all nuclei, at an energy of the order of

$$E_{\text{IVGDR}} \approx 80 A^{-1/3} [\text{MeV}]. \quad (3)$$

At such energies, the wavelength associated with the photons, $\lambda = \frac{hc}{E} \approx 15 A^{1/3}$ fm, is much larger than the nuclear size. The protons feel the effect of an electric field that oscillates rapidly in time but is essentially uniform in space. These conditions correspond to the well-known dipole approximation. Protons are pulled apart from neutrons, and the strong proton-neutron attraction provides the restoring force. This may be seen as a forced harmonic motion: one expects a resonance when the external frequency matches the eigenmode of the system. This is the so-called Isovector Giant Dipole Resonance or IVGDR.

The study of Giant Resonances is a mature field of research, in which many basic facts have been clarified quite some time ago. Monographs exist, that review the classification of these collective modes and illustrate the experimental findings and theoretical methods, established up to the turn of the 20th century (Bortignon et al. (1998); Harakeh and van der Woude (2001)). Consequently, the scope of this chapter is not to start in full detail from scratch. We shall review the basic theory aimed to describe the Giant Resonances and then focus on recent accomplishments and open questions. The emphasis will be on calculations based on Density Functional Theory (DFT) and on *ab initio* approaches in some cases. Purely phenomenological calculations will be mentioned when necessary.

The nuclear ground state and its response to an external field: time-dependent approaches

Let us assume that we can start from a description of the nuclear ground state in terms of independent particles or quasi-particles (Ring and Schuck (1980); Bender et al. (2003)). The single-particle states are solutions of a set of equations of the type

$$h\phi_i = \varepsilon_i\phi_i, \quad (4)$$

where h is an effective Hartree-Fock (HF) or Kohn-Sham (KS) Hamiltonian while ε_i and ϕ_i are the associated eigenvalues and eigenfunctions. The density of the system is, then, given as

$$\rho(\vec{r}) = \sum_{i=1}^F \phi_i^*(\vec{r})\phi_i(\vec{r}). \quad (5)$$

The single-particle states are occupied up to the Fermi level F , and this defines the ground state.

From now on, we shall use the language of second quantisation, where a and a^\dagger are the usual fermionic annihilation and creation operators. The density (5) can be expressed in a generic basis labelled by $i, j \dots$ and its matrix elements read

$$\rho_{ij} = \langle a_j^\dagger a_i \rangle, \quad (6)$$

when evaluated on a state $|\rangle$ of the system under study. Using the HF or KS basis defined by the solution of (4), the density matrix (6) is diagonal if it is evaluated on the HF or KS ground state. Its diagonal matrix elements are, respectively, 1 and 0 for the states below (holes) and above (particles) the Fermi level F . We shall use the standard notation in which h (p) labels a state which is below (above) the Fermi energy and is occupied (empty).

Annihilating a hole and creating a particle is the simplest possible excitation and it is named ‘‘particle-hole’’, or ph : we can write it as $|ph^{-1}\rangle \equiv a_p^\dagger a_h |0\rangle$. These ph excitations can be viewed as small variations of the density matrix around its ground-state value. As we shall discuss, the excitations of the system including the Giant Resonances can be built and understood by using this ph basis. Nuclei having closed shells, that do not display superfluidity, can be described in this manner.

When pairing correlations produce a superfluid ground state, this description is no longer valid. The eigenstates of the system are mixtures of holes and particles, described in terms of the Bogoliubov transformations

$$\alpha_\alpha^\dagger = \sum_i U_{i\alpha} a_i^\dagger + V_{i\alpha} a_i. \quad (7)$$

The states α are called quasi-particle states. The Hartree-Fock-Bogoliubov (HFB) ground state generalises the HF solution: the latter has been defined by $a_p |0\rangle = a_h^\dagger |0\rangle = 0$, whereas the former is defined by $\alpha_\alpha |0\rangle = 0$ for every α . In other words, the HFB ground state is the quasi-particle vacuum, while the HF ground state is the vacuum of particles and holes. The HFB equations, that generalise the HF or KS equations (4), are

$$\begin{pmatrix} h - \lambda & \Delta \\ -\Delta^* & -h^* + \lambda \end{pmatrix} \begin{pmatrix} U_\alpha \\ V_\alpha \end{pmatrix} = E_\alpha \begin{pmatrix} U_\alpha \\ V_\alpha \end{pmatrix}. \quad (8)$$

Here, Δ and λ are the pairing field and Fermi energy, respectively.

In analogy with what we have just discussed in the HF case, the simplest excitations of the system are two quasi-particle excitations (we refer here to excitations that do not change the particle number: a single quasi-particle excitation is an excited state of the $A \pm 1$ system). The density matrix (6) is not sufficient to describe these excitations. We need the so-called pairing tensor as well, which is defined by

$$\kappa_{ij} = \langle a_j a_i \rangle. \quad (9)$$

In order to have a more compact notation, we shall define

$$\mathcal{R} = \begin{pmatrix} \rho & \kappa \\ -\kappa^* & 1 - \rho^* \end{pmatrix}. \quad (10)$$

\mathcal{R} is called generalised density matrix. From its form, we can see that its variations include ph , hh , hp and pp excitations. It can be shown that \mathcal{R} commutes with the HFB Hamiltonian so that, in the basis of the aforementioned quasi-particle states, this matrix is also diagonal and its eigenvalues are equal to either 0 or 1. Another basis, which will be mentioned in what follows, is the canonical basis, in which ρ is diagonal.

Let us now assume that the nucleus is under the action of an external field F . The field gives an initial boost to the nucleus so that wave functions and associated densities are displaced from the equilibrium values. The following time evolution of the generalised density is governed by the equation

$$i\hbar \frac{d}{dt} \mathcal{R} = [\mathcal{H} + F, \mathcal{R}]. \quad (11)$$

In principle, one could solve the time-dependent HFB (TDHFB) equation (11) directly, for instance in coordinate space. The initial condition must be given, and to simulate Giant Resonances one could assume a displacement of all particles, like the shift of protons with respect to neutrons that we have described in the Introduction in the case of the IVGDR. Actually the TDHFB equations are also apt to study large amplitude phenomena. On the other hand, their solution cannot fully describe the features associated with dissipation, like the damping of GRs. The reason is that only the one-body density \mathcal{R} is involved and not the 2-body, 3-body ... A -body densities.

Implementations of TDHFB, or of the simpler time-dependent HF-Bardeen-Cooper-Schrieffer (TDHFBCS) and time-dependent HF (TDHF) approaches, exist. In the case of Skyrme functionals, computer codes have been published in the case of TDHF with only static pairing, and the interested reader can look up the relevant references (Maruhn et al. (2014); Schuettrumpf et al. (2018)) that allow to grasp the details of the solution of the time-dependent equation and also to run examples and learn by direct experience. Other groups have also developed similar approaches and applied them to the study of Giant Resonances (Scamps and Lacroix (2014)). In the past, the semiclassical limit of TDHF, i.e. the Vlasov equation, has been explored [see (Baran et al. (2005)) for a review]. At the moment, this is a tool of choice for the study of intermediate energy reactions, whereas for Giant Resonances there is no big gain in going semiclassical. A recent comparison of RPA, TDHF and Vlasov approaches can be found in (Burrello et al. (2019)). In general, there is full consistency between recent time-dependent and RPA calculations, not only in the case of Skyrme approaches but also in the case of covariant approaches. Relativistic time-dependent Hartree and related approaches are well-established and reviewed, e.g. in (Vretenar et al. (2005)). A computer code has been published in (Berghammer et al. (1995)).

We conclude this discussion with an example of a TDHF calculation for the dipole response of a deformed nucleus, that is displayed in Fig. 1. It has to be noted

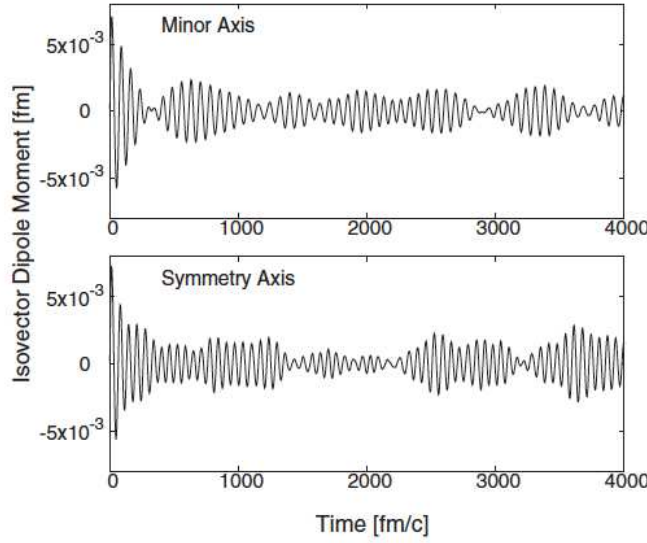


Fig. 1 Dipole moment as a function of time, extracted from a TDHF calculation in the axially symmetric nucleus ^{76}Se . Figure taken from Ref. (Goddard et al. (2013)).

that the GR strength function must be extracted from the time-dependent expectation value of the relevant operator via a Fourier transformation. Consequently, fine details of the strength may not be easily accessible.

Linear response: QRPA and FAM

The further assumption is often made, that the external field F is weak enough so that the response can be written by restricting to lowest order in the density variations that are encoded in \mathcal{R} . In practice, this is the situation that takes place for instance in the case of direct reactions, when the external field acts for a short time regardless of its intrinsic strength (or, to say it better, the experimental findings are often consistent with such a picture).

The weakness of the external perturbation F is consistent with a harmonic time-dependence of the type

$$F(t) = F e^{-i\omega t} + F^\dagger e^{+i\omega t}, \quad (12)$$

where F includes the dependence on space and spin. The wave functions and the generalised density \mathcal{R} (10) will also display changes with the same harmonic dependence:

$$\begin{aligned}\mathcal{R}(t) &= \mathcal{R}^{(0)} + \delta\mathcal{R}(t) \\ \delta\mathcal{R}(t) &= \delta\mathcal{R}e^{-i\omega t} + \delta\mathcal{R}^\dagger e^{+i\omega t},\end{aligned}\quad (13)$$

where $\mathcal{R}^{(0)}$ is the equilibrium value given by (10) evaluated in the HFB ground state. Consequently, the Hamiltonian \mathcal{H} will follow the same harmonic behaviour. In these conditions, and by neglecting higher order terms in F or $\delta\mathcal{R}$ or $\delta\mathcal{H}$, one derives the so-called quasi-particle Random Phase Approximation (QRPA) equations (Khan et al. (2002); Bender et al. (2003)).

In fact, Eq. (11) becomes

$$\begin{aligned}\hbar\omega\delta\mathcal{R} &= [\mathcal{H}^{(0)}, \delta\mathcal{R}] + [\delta\mathcal{H} + F, \mathcal{R}^{(0)}], \\ -\hbar\omega\delta\mathcal{R}^\dagger &= [\mathcal{H}^{(0)}, \delta\mathcal{R}^\dagger] + [\delta\mathcal{H}^\dagger + F^\dagger, \mathcal{R}^{(0)}],\end{aligned}\quad (14)$$

where the upper (lower) line refers to the terms that go like $e^{-i\omega t}$ ($e^{+i\omega t}$). The QRPA set of equations can be obtained from the first line only (the redundancy of the second line could be checked as an exercise). In the above equations the term $[\mathcal{R}^{(0)}, \mathcal{H}^{(0)}]$ vanishes because, as we mentioned in the previous Section, the two matrices can be simultaneously diagonalised in the HFB ground-state. Finally, one can neglect the term in F because the external field plays only the role of an initial boost, as we already alluded to, and does not determine the eigenmodes that are intrinsic properties of the system under study.

The QRPA equations are obtained by taking the matrix elements of the first equation in (14), either between the ground-state $|\tilde{0}\rangle$ and a two quasi-particle state $\alpha_\alpha^\dagger\alpha_\beta^\dagger|\tilde{0}\rangle$, or between the ground-state and $\alpha_\beta\alpha_\alpha|\tilde{0}\rangle$ (the ground-state $|\tilde{0}\rangle$ is more general than the HFB ground state $|0\rangle$). By taking these matrix elements, one finds the following quantities:

$$\begin{aligned}X_{\alpha\beta} &= \langle\tilde{0}|\alpha_\beta\alpha_\alpha\delta\mathcal{R}|\tilde{0}\rangle, \\ Y_{\alpha\beta} &= \langle\tilde{0}|\alpha_\alpha^\dagger\alpha_\beta^\dagger\delta\mathcal{R}|\tilde{0}\rangle,\end{aligned}\quad (15)$$

that are the components of the density variation $\delta\mathcal{R}$ on the two quasi-particle basis. This means that the excited states $|n\rangle$ are here assumed to be

$$|n\rangle = \left(\sum_{\alpha\beta} X_{\alpha\beta}^{(n)} \alpha_\alpha^\dagger \alpha_\beta^\dagger - Y_{\alpha\beta}^{(n)} \alpha_\beta \alpha_\alpha \right) |\tilde{0}\rangle. \quad (16)$$

QRPA can be seen as a linearisation (or a small amplitude limit) of TDHFB: only the amplitudes associated with the simplest excitations, namely two quasi-particle creation and annihilation, are considered. We have put Eq. (16) in a box to stress this hypothesis, and we shall do the same with the following equations of the same kind, so that the reader can appreciate at first sight the various enlargements (or restrictions) of the model space.

The matrix elements of the first line of (14) produce the QRPA equations in their matrix form:

$$\begin{pmatrix} A & B \\ -B^* & -A^* \end{pmatrix} \begin{pmatrix} X \\ Y \end{pmatrix} = \hbar\omega \begin{pmatrix} X \\ Y \end{pmatrix}. \quad (17)$$

The QRPA equations can be written in a simple form if one employs the canonical basis, as the matrix elements become

$$\begin{aligned} A_{\alpha\beta,\gamma\delta} &= (E_{\alpha\gamma} + E_{\beta\delta}) + (u_{\alpha}v_{\beta}u_{\gamma}v_{\delta} + v_{\alpha}u_{\beta}v_{\gamma}u_{\delta}) \langle \alpha\delta | V | \beta\gamma \rangle \\ &\quad + (u_{\alpha}u_{\beta}u_{\gamma}u_{\delta} + v_{\alpha}v_{\beta}v_{\gamma}v_{\delta}) \langle \alpha\beta | V | \gamma\delta \rangle, \end{aligned} \quad (18)$$

$$\begin{aligned} B_{\alpha\beta,\gamma\delta} &= (u_{\alpha}v_{\beta}u_{\gamma}v_{\delta} + v_{\alpha}u_{\beta}v_{\gamma}u_{\delta}) \langle \alpha\delta | V | \beta\gamma \rangle \\ &\quad - (u_{\alpha}u_{\beta}v_{\gamma}v_{\delta} + v_{\alpha}v_{\beta}u_{\gamma}u_{\delta}) \langle \alpha\beta | V | \gamma\delta \rangle. \end{aligned} \quad (19)$$

Here, E is the matrix of the quasi-particle energies already introduced in (8), when written in the canonical basis. In this basis, such matrix is no longer diagonal. The matrices U and V of (7), as well as the pairing tensor (9), assume a simple form in terms only of the coefficients u and v that appear in the previous equation (Ring and Schuck (1980)). Everything becomes even simpler in the BCS approximation, because the quasi-particle basis coincides with the canonical basis and E is also diagonal. Moreover, the v_{α} and u_{α} coefficients are, in this case, the probability amplitudes that the state α is occupied or empty.

Once the QRPA solution is available, with the energies $\hbar\omega_n$ of the states $|n\rangle$ and their wave functions written in terms of the X and Y amplitudes, the strength function (1) can be readily calculated. More details about formulas, together with the complete derivations, can be found in Refs. (Rowe (1970); Ring and Schuck (1980); Suhonen (2007)), where one also finds the expressions in the angular-momentum coupled basis. In the quasi-particle basis, the matrices U and V of the Bogoliubov transformation (7) are not diagonal, and this would make the calculation of the QRPA matrix (17) rather cumbersome.

Even in canonical basis, the matrix in (17) may become very large, especially for heavy and/or deformed nuclei in which spherical symmetry cannot be assumed any longer. This fact has pushed the developments of alternative methods to implement and solve QRPA. In recent years, the so-called finite-amplitude method (FAM) has become increasingly popular.

The FAM has been introduced in (Nakatsukasa et al. (2007)) in the case without pairing, and extended to the case with pairing in (Avogadro and Nakatsukasa (2011)). The starting point is always the time-dependent equation (14) in the linearised or small-amplitude case. The essential trick is that of assuming a generic small variation of \mathcal{R} and calculate the corresponding variation of \mathcal{H} in the form

$$\delta\mathcal{H} = \frac{\mathcal{H}[\mathcal{R}^{(0)} + \eta\delta\mathcal{R}] - \mathcal{H}^{(0)}}{\eta}, \quad (20)$$

where η is a small parameter. It should be noted that this does not require much more effort than a HFB calculation, as one has simply to evaluate the generalised

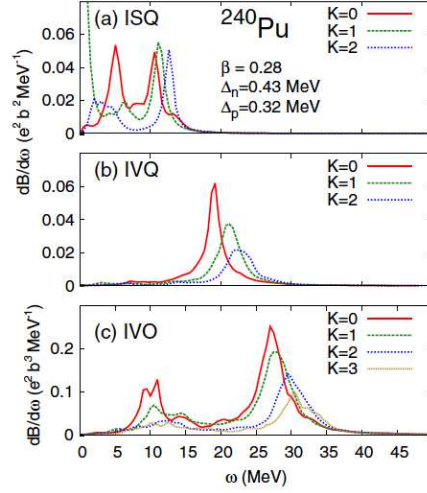


Fig. 2 Isoscalar (a) and isovector (b) quadrupole strengths, and isovector octupole strength (c) in the nucleus ^{240}Pu , calculated with FAM and a Skyrme functional. The figure is taken from Ref. (Kortelainen et al. (2015)), to which we refer for all details.

density and the corresponding Hamiltonian around the ground state, as it is done when seeking for convergence of the HFB equations. In other words, the evaluation of two-body QRPA matrix elements (18) is avoided. By knowing the relation between \mathcal{H} and \mathcal{R} in the linear regime through Eq. (20), one has all the elements to solve Eq. (14). In the papers we have mentioned, this is done by writing this equation on a finite quasi-particle basis. In this way, one turns it into a linear system: given the external field F , the equation can be solved for each value of ω , having as unknowns the values of $\delta\mathcal{R}$ on the chosen basis. The solution of the linear system scales much more favourably than that of a matrix diagonalisation.

In Fig. 2, we show an example of FAM calculation. The multipole strength in a heavy system like ^{240}Pu , with an axial deformation associated with $\beta = 0.28$, would be extremely hard to calculate in a conventional matrix formulation. The formalism has been also implemented with relativistic functionals, and a computer code has been published in Ref. (Bjelčić and Nikšić (2020)).

Reduction to RPA and the schematic model

As we mentioned, in non-superfluid nuclei the HFB solution reduces to the simple HF solution. The u and v coefficients are either 0 or 1, and the pair tensor vanishes. In this condition, QRPA reduces to simple RPA. Eq. (17) keeps the same form while the matrix elements A and B have a simpler form. They reduce to

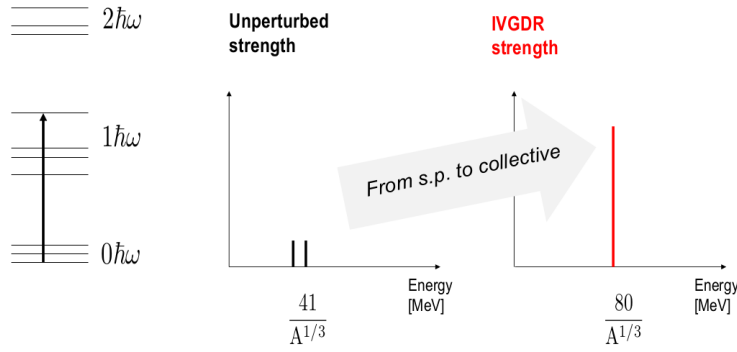


Fig. 3 The schematic TDA model for the IVGDR. In the left panel, the nuclear shells are displayed in order to emphasise their alternate parity and the fact that we expect the IVGDR to be made by particle-hole excitations at $\approx l\hbar\omega$. In the central and right panels, we draw the unperturbed and TDA strength $S(E)$, respectively. See the text for a discussion.

$$A_{ph,p'h'} = +\delta_{pp'}\delta_{hh'}(\varepsilon_p - \varepsilon_h) + \langle ph'|V|hp'\rangle, \quad (21)$$

$$B_{ph,p'h'} = \langle pp'|V|hh'\rangle, \quad (22)$$

where ε are the single-particle energies that we have introduced in (4). The matrix elements that enter the strength function (1) can be calculated from

$$\langle n|F|0\rangle = \sum_{ph} (X_{ph} + Y_{ph}) \langle p|F|h\rangle. \quad (23)$$

As in the case of QRPA, the reader can find details and formulas written with proper angular momentum coupling in the general references that have been quoted above.

The B matrix elements, and the associated Y amplitudes are very important to describe the low-lying excitations like 2^+ and 3^- in spherical nuclei, but turn out to be less important for high-energy states like the GRs. Neglecting the B -sector of the RPA matrix leads to the so-called Tamm-Dancoff approximation or TDA. We will now see how a schematic TDA model accounts for the existence of collective modes like the IVGDR, in a pedagogical and transparent manner.

To this aim, let us assume that we have N degenerate p-h excitations at energy ε . In the case of the IVGDR, which has $J^\pi = 1^-$, this corresponds to a large extent to holes in the highest occupied shell and particles in the lowest unoccupied shell. Consequently, ε will be $\approx l\hbar\omega \approx 41 A^{-1/3}$, as emphasised by the vertical arrow in the left panel of Fig. 3.

We also consider the matrix elements that appear in A as being all equal to a constant v . The TDA matrix becomes:

$$\begin{pmatrix} \varepsilon + v & v & \dots & v \\ v & \varepsilon + v & \dots & v \\ \dots & & & \dots \\ v & v & \dots & \varepsilon + v \end{pmatrix}. \quad (24)$$

Such simple model is exactly solvable. In the two by two case the matrix reads

$$\begin{pmatrix} \varepsilon + v & v \\ v & \varepsilon + v \end{pmatrix}, \quad (25)$$

and the eigenvalues and eigenvectors are

$$\begin{aligned} \hbar\omega_1 &= \varepsilon, & X^{(1)} &= \frac{1}{\sqrt{2}} \begin{pmatrix} 1 \\ -1 \end{pmatrix}, \\ \hbar\omega_2 &= \varepsilon + v, & X^{(2)} &= \frac{1}{\sqrt{2}} \begin{pmatrix} 1 \\ 1 \end{pmatrix}. \end{aligned} \quad (26)$$

We may call ‘‘incoherent’’ the first state because the two amplitudes have opposite phase, whereas the second state may be said to be ‘‘coherent’’. This wording will become clearer if we calculate the matrix elements defined by Eq. (23):

$$\langle n|F|0\rangle = \sum_{ph} X_{ph} \langle p|F|h\rangle. \quad (27)$$

Consistently with the assumptions that have been already made, we can approximate the matrix elements $\langle p|F|h\rangle$ with a constant number M . Then, if one takes the incoherent state, the transition amplitude (27) associated with F vanishes. Instead, its value is increased by a factor $\sqrt{2}$ with respect to the ‘‘single-particle value’’ M in the coherent case.

The schematic TDA equation (24) can also be solved in the general case with N ph transitions. Also in that case, one finds there is only one coherent state, characterised by an eigenvalue $\varepsilon + Nv$ and by a corresponding eigenvector of the type

$$\frac{1}{\sqrt{N}} \begin{pmatrix} 1 \\ 1 \\ \dots \\ 1 \end{pmatrix}. \quad (28)$$

The transition amplitude (27) becomes

$$\langle n|F|0\rangle = \sum_{ph} X_{ph} \langle p|F|h\rangle \approx N \frac{1}{\sqrt{N}} M = \sqrt{N} M. \quad (29)$$

The quantity that appears in the strength function (1) is the square of the transition amplitude, that is

$$|\langle n|F|0\rangle|^2 = N M^2. \quad (30)$$

In the case of the IVGDR, we clearly see that the term $N\nu$ shifts the coherent eigenvalue from the unperturbed value $\varepsilon \approx 41 \text{ A}^{-1/3}$ to the value $80 \text{ A}^{-1/3}$ already mentioned in Eq. (3). The fact that this is a “giant”, or collective, state is highlighted by Eq. (30): its probability to be excited by the external field becomes N times larger than the typical probability M^2 of a single-particle state. The situation is depicted in Fig. 3. In the central panel, we show the hypothetical single-particle, or unperturbed, strength at energy ε , which is made by several peaks whose height is M^2 . In the right panel, we display instead the Giant Resonance made by a single peak whose height is larger by the factor N . Schematic models have been widely introduced throughout the years to describe collective states, and not only the IVGDR, starting from the seminal work of Ref. (Brown and Bolsterli (1959)).

Operators and example of calculations

The GRs are excited by external operators that are classified as follows (Harakeh and van der Woude (2001)). In the non spin-flip case (electric GRs), the operators F associated with different values of the transferred angular momentum L read

$$F_{\text{IS}} = \sum_i r_i^L Y_{LM}(\hat{r}_i), \quad (31)$$

$$F_{\text{IV}} = \sum_i r_i^L Y_{LM}(\hat{r}_i) \tau_z(i). \quad (32)$$

In this way, we clearly distinguish isoscalar (IS) from isovector (IV) modes, that is, cases in which protons and neutrons oscillate in phase from cases in which they move against each other. Y_{LM} are the usual spherical harmonics and \hat{r} is, here and in what follows, a shorthand notation for the polar angles of \vec{r} . Values of $L = 0, 1, 2, 3, \dots$ correspond to monopole, dipole, quadrupole, octupole \dots resonances. It is important to notice that the radial factor r^L must be thought as the limit of the Bessel function $j_L(qr)$ when qr goes to zero (cf. the discussion in the next Section). When this term becomes meaningless, one must consider the next term in the Taylor expansion of the Bessel function, that is r^{L+2} . For instance, in the monopole case, Y_{00} is a constant that can be neglected and the operator becomes

$$F_{\text{ISGMR}} = \sum_i r_i^2, \quad (33)$$

$$F_{\text{IVGMR}} = \sum_i r_i^2 \tau_z(i). \quad (34)$$

The other case in which the term r^L does not act as an excitation operator is the isoscalar dipole case. $rY_{1M}(\hat{r})$ can be shown to produce a translation of the whole nucleus, and also in this case the relevant operator becomes proportional to r^{L+2} , namely

$$F_{\text{ISGDR}} = \sum_i r_i^3 Y_{1M}(\hat{r}_i). \quad (35)$$

The nuclear translation, i.e. the motion of the nuclear centre of mass, should appear at zero excitation energy in an exact calculation, and should be decoupled from the physical excitation modes. However, if this decoupling is not exactly realised, a way to avoid the contamination of the physical ISGDR strength by the spurious translational strength, consists in employing the modified operator (Van Giai and Sagawa (1981))

$$F_{\text{ISGDR}} = \sum_i (r_i^3 - \eta r_i) Y_{1M}(\hat{r}_i), \quad (36)$$

where $\eta = \frac{5}{3} \langle r^2 \rangle$.

In addition to isoscalar and isovector operators, one could be interested in the electromagnetic excitation processes. In this case, the excitation operators become

$$F_{\text{e.m.}} = e \sum_i r_i^L Y_{LM}(\hat{r}_i) (1 - \tau_z(i)). \quad (37)$$

In the dipole case, it is customary to remove the contribution from the centre of mass, so that the IVGDR electromagnetic operator becomes

$$F_{\text{IVGDR}} = \frac{eN}{A} \sum_{i=1}^Z r_i Y_{1M}(\hat{r}_i) - \frac{eZ}{A} \sum_{i=1}^N r_i Y_{1M}(\hat{r}_i). \quad (38)$$

The effective charge for protons (neutrons) turns out to be $\frac{eN}{A}$ ($-\frac{eZ}{A}$). In principle, this subtraction of the centre of mass should be done for every multipole. However, for $L \geq 2$, the resulting effective charges do not differ significantly from 1 and 0 [see their expression, e.g. on p. 98 of Ref. (Eisenberg and Greiner (1976))].

In the spin-flip case (magnetic GRs) we write, in a similar way as in (31) and (32),

$$F_{\text{IS}} = \sum_i r_i^L [Y_{LM}(\hat{r}_i) \otimes \vec{\sigma}(i)]_J, \quad (39)$$

$$F_{\text{IV}} = \sum_i r_i^L [Y_{LM}(\hat{r}_i) \otimes \vec{\sigma}(i)]_J \tau_z(i). \quad (40)$$

As we said, J^π are good quantum numbers; but, as far as the operators are concerned, we are considering also L and S as approximate quantum numbers.

The operators (32) and (40) correspond to transitions within the same nucleus. There exist charge-exchange GRs, that correspond to the case in which the operator τ_z is replaced by τ_\pm . The excited states of a given nucleus are, then, in the neighbouring $Z \mp 1$ isotopes: these are states that can be populated by β -decay, if energetically possible, plus those at higher energy. In what follows, we will show examples of strength functions in the case of the Gamow-Teller Resonance (GTR), that is for the operator (40) in the case $L = 0$,

$$F_{\text{GTR}} = \sum_i \sigma_\mu(i) \tau_-(i). \quad (41)$$

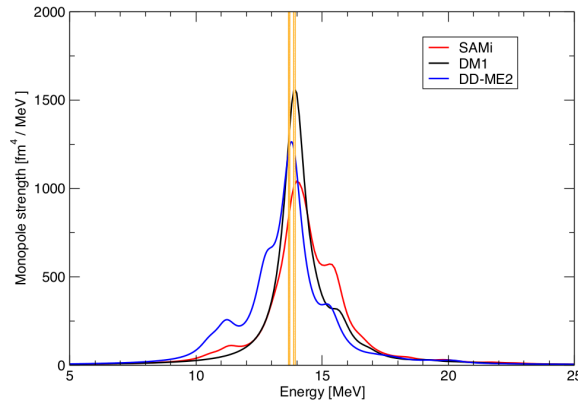


Fig. 4 RPA calculations of the monopole strength in ^{208}Pb , performed by using the nonrelativistic Skyrme-type functional SAMi (Roca-Maza et al. (2012)), the Gogny-type functional DM1 (Goriely et al. (2009)), and the relativistic functional DDME2 (Lalazissis et al. (2005)). The discrete RPA peaks are smeared out with Lorentzian functions having a width of 1 MeV [Eq. (2) is used with a fixed width]. The vertical lines show the peak energy obtained in the experiments performed at TAMU (13.9 MeV) and RCNP (13.7 MeV). Figure taken from (Garg and Colò (2018)), where the original references for the experimental data can be found.

We display in this Section some realistic examples of RPA and QRPA calculations. In Fig. 4, one can see the results of RPA calculations of the ISGMR in the spherical nucleus ^{208}Pb , performed with different EDFs, of Skyrme, Gogny and covariant type. The figure is meant to illustrate the fact that RPA can reproduce well the experimental value of the ISGMR peak energy, provided the Hamiltonian or EDF is well calibrated. In this case, the different EDFs are all associated with a realistic value of the nuclear incompressibility K_∞ , and the result does not depend much on whether a Skyrme, Gogny or covariant functional is used.

In Fig. 5, we show QRPA calculations of the ISGMR that have been performed without assuming spherical symmetry along the chain of the Mo isotopes. These isotopes display a modest deformation which is enough, nonetheless, to produce an observable effect. In fact, for axially deformed nuclei only the projection of J along the symmetry axis, called K , is a good quantum number. The calculations are performed in a space with good K^π , so that the monopole states are coupled to the $K = 0$ component of the quadrupole states (in principle, they are coupled also with higher multipoles but this coupling becomes significantly smaller with increasing angular momentum). The monopole-quadrupole coupling is evident from Fig. 5. The use of operators of the type $F = r^L Y_L$ helps to partially decouple the multipoles (Arteaga and Ring (2008)), but a full angular momentum projection would be called for. Similar calculations have been performed by other groups [cf. (Yoshida (2021)) and references therein].

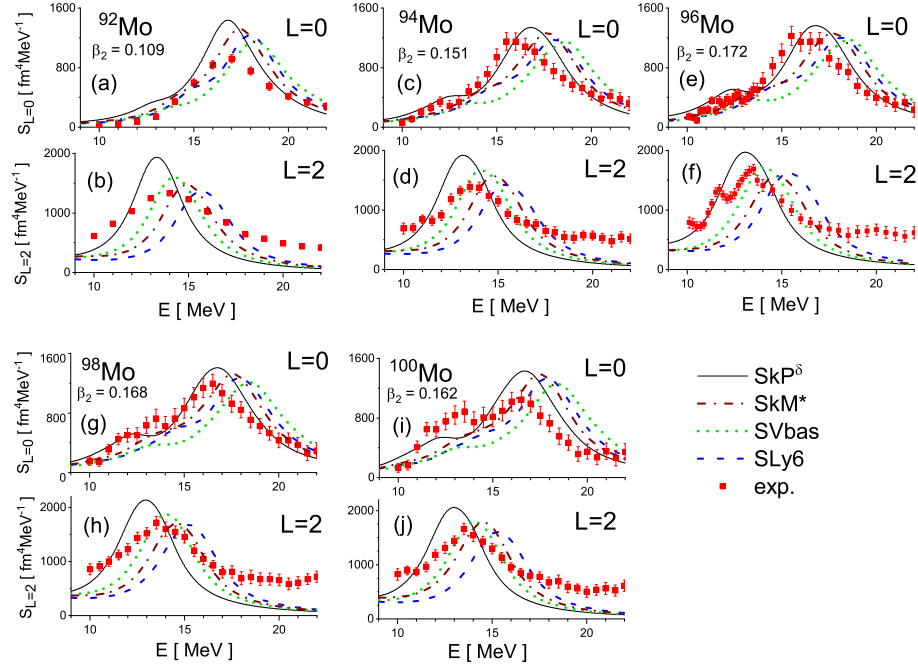


Fig. 5 Isoscalar monopole and quadrupole strengths in $^{92,94,96,98,100}\text{Mo}$, calculated within QRPA and using the Skyrme forces SkM*, SLy6, SVbas and SkP $^\delta$. The strengths are compared with the experimental data. The figure is taken from (Colò et al. (2020)), where references to the experimental data and details on the method used can be found.

Relationship between strength functions and inelastic cross sections

State-of-the-art reaction calculations are performed within the so-called Distorted-Wave Born Approximation (DWBA), in which the differential cross section is given by

$$\frac{d\sigma}{d\Omega} = \frac{k_f}{k_i} |f(\theta)|^2 = \frac{\mu^2 k_f}{4\pi^2 \hbar^4 k_i} \left| \int d^3R \chi_{k_f}^*(\mathbf{R}) \langle f|V|i\rangle \chi_{k_i}(\mathbf{R}) \right|^2. \quad (42)$$

Here, V is a projectile-target interaction and χ are the distorted waves in the initial and final channels, in which the relative motion is associated with the momenta k_i and k_f , respectively. In what follows, we will assume $k_f \approx k_i$. \mathbf{R} is the relative projectile-target coordinate and μ is the reduced mass. Although in inelastic scattering the mutual interaction V can act as a field to excite one of the two nuclei, Eq. (42) does not display any simple relationship with the strength function that we have discussed so far.

To unveil this relationship, we are obliged to drastically simplify our formulation. We resort to the Plane-Wave Born Approximation (PWBA) and we assume that the

interaction V is a zero-range force. Within the PWBA, if \mathbf{q} is the momentum transfer, the scattering amplitude $f(\theta)$ is simply

$$\begin{aligned} f(\theta) &= -\frac{\mu}{2\pi\hbar^2} \int d^3R e^{i\mathbf{q}\cdot\mathbf{R}} \langle f|V|i\rangle \\ &= -\frac{2\mu}{\hbar^2} \sum_{LM} i^L \int d^3R j_L(qR) Y_{LM}(\hat{R}) Y_{LM}^*(\hat{q}) \langle f|V|i\rangle, \end{aligned} \quad (43)$$

where we have used the expansion of the plane wave in spherical components. Accordingly, we also expand in multipoles the interaction V , and we neglect its spin- and isospin-dependence for the sake of simplicity:

$$V \equiv \sum_i V(\mathbf{R} - \mathbf{r}_i) = V_0 \sum_i \delta(\mathbf{R} - \mathbf{r}_i) = V_0 \sum_i \sum_{\lambda\mu} \frac{\delta(R - r_i)}{R^2} Y_{\lambda\mu}(\hat{r}_i) Y_{\lambda\mu}^*(\hat{R}). \quad (44)$$

We insert Eq. (44) in (43) and we obtain

$$f(\theta) = -\frac{2\mu V_0}{\hbar^2} \sum_{LM} i^L Y_{LM}^*(\hat{q}) \sum_i \langle f|j_L(qr_i) Y_{LM}(\hat{r}_i)|i\rangle. \quad (45)$$

In case of experiments with unpolarised beams, in order to obtain the cross section, we have to average over the possible values of M of the initial state and sum over the values of M of the final state. This is simple in the case of $L = 0$ initial state, where the final M -value and the transferred M of Eq. (45) coincide. Eventually, for a given L -transfer,

$$\frac{d\sigma}{d\Omega} = \left(\frac{2\mu V_0}{\hbar^2} \right)^2 \frac{|\langle f||j_L Y_L||i\rangle|^2}{4\pi} P_L(\cos(\theta)), \quad (46)$$

where P_L is a Legendre polynomial. If the momentum transfer q is small enough so that the condition $qR \ll 1$ holds, we can exploit the fact that the Bessel functions behave as $j_L(qR) \approx (qR)^L$. In this case, one can see clearly that the cross section (46) factorises into a kinematical part and the square of the matrix element of the operators that we have already displayed in Eq. (31), that are those commonly used in RPA and its extensions.

We stress, once again, that this decomposition into a kinematical factor and the square of the matrix element of a radial multipole operator is valid only within the plane-wave approximation. In reality, the cross section will be “distorted” with respect to the strength function. However, the relationship that we have highlighted possesses its conceptual validity as a guideline.

More general frameworks beyond (Q)RPA

The natural extension of QRPA is second QRPA, in which the excited states are supposed to have not only two quasi-particle components but also four quasi-particles components,

$$|N\rangle = \left(\sum_{\alpha\beta} X_{\alpha\beta}^{(1)} \alpha_{\alpha}^{\dagger} \alpha_{\beta}^{\dagger} - Y_{\alpha\beta}^{(1)} \alpha_{\beta} \alpha_{\alpha} + \sum_{\alpha\beta\gamma\delta} X_{\alpha\beta\gamma\delta}^{(2)} \alpha_{\alpha}^{\dagger} \alpha_{\beta}^{\dagger} \alpha_{\gamma}^{\dagger} \alpha_{\delta}^{\dagger} - Y_{\alpha\beta\gamma\delta}^{(2)} \alpha_{\delta} \alpha_{\gamma} \alpha_{\beta} \alpha_{\alpha} \right) |\tilde{0}\rangle. \quad (47)$$

In the non-superfluid case second QRPA reduces to second RPA (SRPA), and the states $\alpha\beta$ and $\alpha\beta\gamma\delta$ are replaced by ph and $php'h'$, respectively. With a procedure similar to that outlined in our previous discussion, the SRPA equations can be obtained by demanding that the eigenstates of the system have the more general form (47) instead of the simpler form (16). Their derivation can be found in textbooks like (Rowe (1970)) [cf. also (Yannouleas (1987)) and the more recent (Papakonstantinou (2014)) for their formal properties]. One should note that the SRPA ground-state is still more general than the ground-state $|\tilde{0}\rangle$ that we have discussed in the paragraph above Eq. (16); nevertheless, we have avoided to introduce a more complicated notation.

The SRPA equations can be cast in a matrix form, that is,

$$\begin{pmatrix} A_{11} & A_{12} & B_{11} & B_{12} \\ A_{21} & A_{22} & B_{21} & B_{22} \\ -B_{11}^* & -B_{12}^* & -A_{11}^* & -A_{12}^* \\ -B_{21}^* & -B_{22}^* & -A_{21}^* & -A_{22}^* \end{pmatrix} \begin{pmatrix} X^{(1)} \\ X^{(2)} \\ Y^{(1)} \\ Y^{(2)} \end{pmatrix} = \hbar\omega \begin{pmatrix} X^{(1)} \\ X^{(2)} \\ Y^{(1)} \\ Y^{(2)} \end{pmatrix}. \quad (48)$$

In fact, this equation is analogous to (17), except for the fact that the matrices A and B have larger dimension. The indices 1 and 2 refer to the part of the model space that includes 1p-1h and 2p-2h configurations, respectively. As discussed in (Yannouleas (1987)), the expressions of A and B can be obtained after a lengthy but straightforward calculation. The detailed formulas are not reported here but we stress that A and B_{11} do not vanish, whereas $B_{21} = B_{12} = B_{22} = 0$.

If we use standard projection techniques to reduce (48) to an equivalent equation in the smaller 1p-1h space, we find

$$\begin{pmatrix} \mathcal{A}(\omega) & \mathcal{B} \\ -\mathcal{B}^* & -\mathcal{A}^*(-\omega) \end{pmatrix} \begin{pmatrix} \mathcal{X} \\ \mathcal{Y} \end{pmatrix} = \hbar\omega \begin{pmatrix} \mathcal{X} \\ \mathcal{Y} \end{pmatrix}, \quad (49)$$

where

$$\begin{aligned} \mathcal{A}(\omega) &= A_{11} + \Sigma(\omega), \\ \mathcal{B} &= B_{11}, \end{aligned} \quad (50)$$

and Σ is the self-energy of the 1p-1h configurations due to the coupling with 2p-2h,

$$\Sigma(\omega) = A_{12} \frac{1}{\hbar\omega - A_{22}} A_{21}. \quad (51)$$

Although SRPA has been proposed as a theory a long time ago, during several decades calculations were too demanding especially for medium-heavy nuclei. One of the most common approximations that have been adopted, consisted in assuming the 2p-2h states as non interacting. In this way, the matrix A_{22} is diagonal and the computational effort is not much heavier than RPA [Eq. (51) contains only a sum]. This is called indeed “diagonal approximation”. More recently, realistic SRPA calculations that lift this severe approximation have been performed.

SRPA can be presently performed even with realistic interactions, as demonstrated in (Papakonstantinou and Roth (2010)). The quality of the results, in terms of favourable comparison with experiment, depends on the adopted Hamiltonian. In fact, we should mention an interesting key open question at this point. The self-energy (51) is an increasing function of ω , that tends to shift a significant amount of strength downward in energy. In the case of a zero-range interaction like the Skyrme one, the self-energy does actually diverge if ω becomes arbitrarily large. But even with finite-range interactions like Gogny, the accumulation of low-energy strength that was found in SRPA calculations [see, e.g., (Gambacurta et al. (2015))] was found to be unrealistically large and in contrast with the experimental findings. This may be related to the Hamiltonian or EDF that is employed and/or may be reduced by introducing further correlations beyond SRPA.

Definitely, effective Hamiltonians or EDFs are fitted at mean-field level. When practitioners check if the Hamiltonian of EDF is “well calibrated” for the GR sector (as we mentioned when discussing that EDFs provide a correct ISGMR energy if associated with the correct value of K_∞), they do it at the level of RPA. SRPA (as is also true for the models to be introduced below) produces an additional shift of the states $|N\rangle$ of (47) towards lower energies, in addition to broadening the strength and making it more fragmented because the states $|N\rangle$ are many more than the RPA states. In Ref. (Tselyaev (2013)), it has been argued that, in order to include effects beyond mean-field without altering the properties that a sensible EDF must keep, one has to implement SRPA using the so-called “subtraction technique”. This means replacing, in Eq. (50),

$$\Sigma(\omega) \rightarrow \Sigma(\omega) - \Sigma(\omega = 0). \quad (52)$$

This prescription avoids also possible divergences of the self-energy (to be definitely expected in the case of zero-range forces) when the upper limit on the energy of the 2p-2h states is increased. On the other hand, its grounds in a general many-body theory, as well as its implications for other studies like the shift and fragmentation of the single-particle strength, have not been yet fully clarified. We show in Fig. 6 an example of a recent calculation using the subtraction technique, labelled as subtracted-SRPA or SSRPA.

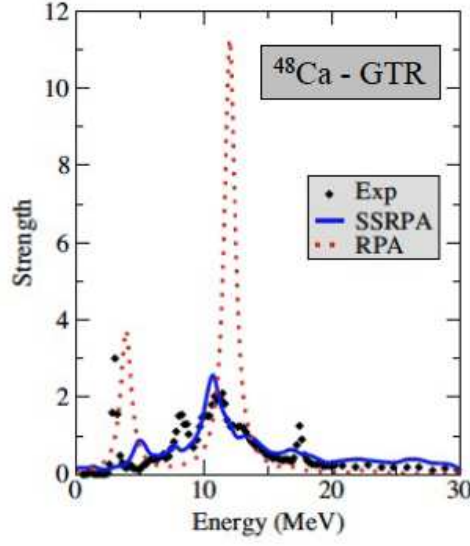


Fig. 6 Gamow-Teller strength in ^{48}Ca calculated in RPA and SRPA with subtraction (SSRPA), using the Skyrme interaction SGII. Figure taken from (Gambacurta et al. (2020)), where details and the reference to the experimental data can be found.

In (Q)RPA plus particle-vibration coupling [(Q)RPA+PVC], one adpots a similar philosophy as in SRPA but the four quasi-particle (or 2p-2h) states are replaced by two quasi-particles (or 1p-1h) plus a vibration or phonon. This means that Eq. (47) becomes

$$|N\rangle = \left(\sum_{\alpha\beta} X_{\alpha\beta}^{(1)} \alpha_{\alpha}^{\dagger} \alpha_{\beta}^{\dagger} - Y_{\alpha\beta}^{(1)} \alpha_{\beta} \alpha_{\alpha} + \sum_{\alpha\beta n} X_{\alpha\beta n}^{(2)} \alpha_{\alpha}^{\dagger} \alpha_{\beta}^{\dagger} \Gamma_n^{\dagger} - Y_{\alpha\beta n}^{(2)} \Gamma_n \alpha_{\beta} \alpha_{\alpha} \right) |\tilde{0}\rangle, \quad (53)$$

where Γ_n^{\dagger} is the creator of the QRPA state $|n\rangle$ in (16), that is

$$\Gamma_n^{\dagger} = \sum_{\alpha\beta} X_{\alpha\beta}^{(n)} \alpha_{\alpha}^{\dagger} \alpha_{\beta}^{\dagger} - Y_{\alpha\beta}^{(n)} \alpha_{\beta} \alpha_{\alpha}. \quad (54)$$

The rationale behind this choice is that, by replacing a pair of quasi-particles with one vibration, one includes further correlations.

More specifically, the vibrational states $|n\rangle$ lie, on average, at lower energy than the two quasi-particle states. In other words, the states labelled by $\alpha\beta n$ in (53) lie, on average, at lower energy than the states labelled by $\alpha\beta\gamma\delta$ in (47). Either class of states is commonly referred to with the wording “doorway states”: they constitute the “doorway” to GR damping. The doorway states that lie at lower energies are

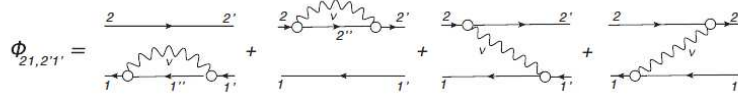


Fig. 7 The so-called “dynamical kernel” of the Time-Blocking Approximation (TBA). See the text for a short discussion. Figure taken from (Litvinova and Schuck (2019a)).

more likely to be coupled to the dominant two quasi-particle components: therefore, (Q)RPA+PVC is more effective in reproducing the GR widths than SRPA. On the other hand, the doorway states that appear in (Q)RPA+PVC form an overcomplete basis and violate, to some extent, the Pauli principle while the same does not happen in SRPA. We will discuss further this issue here below.

The first implementation of this model using Skyrme interactions has been described in detail in (Colò et al. (1994)). The same model has been resumed in (Roca-Maza et al. (2017)) for non charge-exchange states and in (Niu et al. (2014)) for charge-exchange states. All these calculations can be understood along the same line of the discussion made for SRPA. A matrix which is fully comparable to (49) is diagonalised, and the self-energy is also analogous to that of SRPA in the diagonal approximation. Eq. (51) holds, but it includes the coupling of 1p-1h to 1p-1h plus a phonon n . By writing it in detail, we obtain

$$\Sigma_{ph,p'h'}(\omega) = \sum_{p''h''n} A_{ph,p''h''n} \frac{1}{\hbar\omega - (\varepsilon_{p''} - \varepsilon_{h''} + \hbar\omega_n)} A_{p''h''n,p'h'}. \quad (55)$$

In Ref. (Shen et al. (2020)), the approximation of completely non-interacting 1p-1h-1 phonon states has been removed. All these works deal with the implementation without pairing. QRPA+PVC for non charge-exchange states has been introduced, using Skyrme Hamiltonians and based on HF-BCS, in Ref. (Colò and Bortignon (2001)). More recently, QRPA+PVC for charge-exchange states on the HFB basis has been introduced in (Niu et al. (2016)). In all these works, an overall satisfactory description of the lineshape of GRs, namely of their width and fragmentation, has been achieved.

There is quite a strict relationship between (Q)RPA+PVC and the Time-Blocking Approximation (TBA). This theory has been introduced in the context of phenomenological calculations based on a Woods-Saxon mean-field plus a residual Landau-Migdal interaction (Kamerdzhev et al. (2004)). Nevertheless, there exists a series of recent GR calculations using Skyrme functionals [cf. Tselyaev et al. (2016) and references therein]. In the basic version, TBA is actually the same framework as the one we have just described under the name of (Q)RPA+PVC. In Fig. 7, we depict the Feynman diagrams that correspond to the so-called “dynamical kernel” of this theory. These diagrams correspond, in fact, to the coupling between states 12 and $1'2'$ belonging to the two quasi-particle space with intermediate doorway states given by 1p-1h plus a phonon v . Thus, the quantity Φ in Fig. 7 is exactly the self-energy $\Sigma(\omega)$ of Eq. (55). In the calculations reported in Ref. (Tselyaev et al.

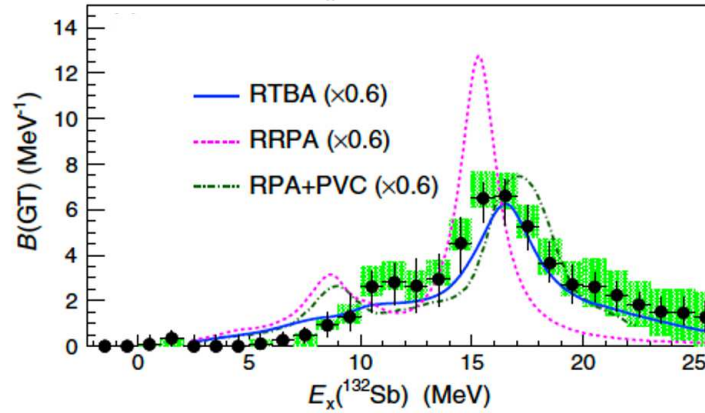


Fig. 8 Gamow-Teller strength in ^{132}Sn . The experimental data and the figure are taken from (Yasuda et al. (2018)), where more details can be found. The figure shows a comparison of the performance of different theoretical approaches discussed in this chapter.

(2016)), the coupling to the continuum is to some extent included [as it was in (Colò et al. (1994))]. The description of the width of the GRs in magic, medium-heavy nuclei is rather good, although this is less true in light nuclei as ^{16}O . Whether this is due to missing decay channels like the α -particle decay, or to other limitations of the model, is still unclear.

In Fig. 8, we show results for a case in which we can compare simple relativistic RPA (RRPA), in which a small width is put by hand, with relativistic TBA (RTBA) and RPA+PVC. The differences between these last two approaches should be ascribed to the different functionals employed. RTBA has been introduced in Refs. (Litvinova et al. (2007)) and (Litvinova et al. (2008)) for magic and superfluid nuclei, respectively. Recently, progress has been made in pushing this theory beyond the level we have described in this Section. In the work of Ref. (Robin and Litvinova (2019)), on top of the diagrams already depicted in Fig. 7, further ones of second-order in the particle-phonon interaction have been introduced in the self-energy $\Sigma(\omega)$. Even more interestingly, RTBA has been recast as a specific approximation within the general many-body theory in Ref. (Litvinova and Schuck (2019a)) [cf. also Ref. (Litvinova and Schuck (2020)) for the superfluid case].

In all the models based on the interplay of particles and vibrations, or phonons, one of the issues is the number of phonons included and the convergence of the results with respect to this input. In this respect, the convergence of the GR peak energy with respect to the model space has been carefully studied in (Tselyaev et al. (2016)). The convergence with respect to the maximum phonon energy is well realised; on the other hand, regarding the phonon strength, the problem is that there is moderate dependence (optimistically, a sort of plateau) when one decreases the cut-off strength of the phonon to about 10%. It has to be noted that introducing phonons with small values of strength, i.e. non collective, raises the issue of the Pauli princi-

ple violations that we have already mentioned. In principle, in all the theories that we have discussed, precise prescriptions exist to restore the Pauli principle; in practice, however, exact prescriptions are seldom used and practitioners often employ a practical recipe that consists in using only collective phonons.

We end this Section by mentioning another model that shares a similar point of view. The Quasiparticle-Phonon Model (QPM) describes GRs as admixtures of one phonon components, two phonons components, etc. The single phonon is built using QRPA, that is, the phonon creation operator is given by Eq. (54). The equation corresponding to (47) or to (53) reads

$$|N\rangle = \sum_n R_n \Gamma_n^\dagger + \sum_{nn'} P_{nn'} \Gamma_n^\dagger \Gamma_{n'}^\dagger |\tilde{0}\rangle, \quad (56)$$

where R_n and $P_{nn'}$ are unknown amplitudes to be determined. The basic theory can be found in (Soloviev (1992)). Within the QPM, detailed equations to correct for the Pauli principle violations have been written and, to a large extent, implemented. On the other hand, QPM has been mostly implemented using phenomenological input (a Woods-Saxon mean-field plus schematic pairing and a separable residual interaction). Among the countless applications of QPM to the analysis of GRs, we single out the studies of double GRs [cf. (Ponomarev et al. (2000, 2001)) and references therein], and the analysis of the low-lying pygmy dipole strength and its IS/IV character (Savran et al. (2008); Endres et al. (2010)).

Width, fine structure, particle- and γ -decay

We have already discussed the width of GRs in the previous sections. The purpose of this specific and short section is to distinguish more carefully the different contributions to that width, and discuss the capability of the different approaches to describe each of them. Again, the topic is not new and, in addition to the general textbooks, we should quote the review paper (Bertsch et al. (1983)).

(Q)RPA and the related approaches can account for the fact that there is not a single GR peak but the strength is instead fragmented (cf. the different figures in this chapter and, in particular, Fig. 5). This fragmentation is, at times, referred to as the so-called ‘‘Landau width’’; but this wording is somehow ambiguous and ought to be better avoided. The total width Γ is, then, given by the following terms:

$$\Gamma = \Gamma^\uparrow + \Gamma^\downarrow + \Gamma_\gamma. \quad (57)$$

The so-called ‘‘escape width’’ Γ^\uparrow is associated with the coupling to the continuum, that is, to the emission of particles. GRs are, as a rule, above the threshold for particle emission and can emit most likely neutrons but also protons and, in some cases, heavier residues like α -particles. Continuum-RPA (CRPA) is the model in which one considers p-h excitations with the particle in the continuum part

of the spectrum, without the discretisation that is implicit in equations like (17), (21) and (22). At the turn of the 20th century, a series of works have implemented CRPA fully self-consistently using Skyrme functionals: the purpose was the analysis of GRs and low-energy multipole strength in exotic nuclei close to the drip line (Hamamoto et al. (1997a), Hamamoto et al. (1997b), Hamamoto et al. (1998)). Later, CRPA has been implemented also in the case of finite-range effective interactions like Gogny, both for normal (De Donno et al. (2011)) and charge-exchange excitations (De Donno et al. (2016)).

To disentangle the escape width from the other contributions in (57), one has to measure the emitted particles. Experimental measurements of particle-decay are described in textbooks (Harakeh and van der Woude (2001)). Both phenomenological [see (Gorelik et al. (2021)) and numerous references therein] and fully microscopic approaches (Colò et al. (1994)) have been proposed to calculate the partial decay widths Γ_c^\uparrow (c labels a specific decay channel and by definition $\Gamma^\uparrow = \sum_c \Gamma_c^\uparrow$).

Γ^\downarrow is the so-called “spreading width”. While Γ^\uparrow is associated with the damping into external degrees of freedom, Γ^\downarrow is associated with the damping into internal degrees of freedom. In other words, the spreading width corresponds to the finite lifetime with which the simple configurations, like two quasi-particles, decay into progressively more complex degrees of freedom like four quasi-particles, six quasi-particles etc. (In magic nuclei, we would speak about 1p-1h that decay into 2p-2h, 3p-3h etc.) Except in light nuclei, Γ^\downarrow is by far dominant (Bertsch et al. (1983)). All the models that we have described in the last Section (SRPA, QRPA+PVC, TBA and beyond, QPM) are based on, and support, the idea that most of the damping is accounted for by the coupling at the level of 2p-2h. The effect of 3p-3h coupling on the GRs is arguably small (Ponomarev et al. (1996)).

Recently, a series of high-resolution experiments have been carried out, with the goal of understanding the underlying structure of the GR line shape. The question can be asked, whether the GRs are best described as single Lorentzians with a large width, or in terms of more complicated structures. To this aim, the so-called wavelet analysis has been carried out by looking both at experimental strength functions or cross sections, and at the theoretical results [cf. (Shevchenko et al. (2004)) and references therein]. The conclusion, so far, is that similar scales appear in experiment and theory although quantitative differences show up when one compares them in detail. The idea that coupling at the level of 2p-2h is the dominant mechanism seems to be supported by this analysis in different cases, like dipole and quadrupole resonances.

Finally, Γ_γ in Eq. (57) is a very tiny contribution, of the order of $10^{-3} - 10^{-4}$ of the total width. The direct γ -decay is, nevertheless, a further probe of the microscopic structure of GRs, as the other observables that we have discussed in this Section like the fine structure and the particle emission. The γ -decay of GRs to the ground state can be calculated within (Q)RPA. In principle, electromagnetic transitions from the GR to another phonon state could be also calculated at the (Q)RPA level, but this goes against the fact that (Q)RPA as a framework includes only lowest order processes. Calculations at the level of QPM and RPA+PVC have

been reported, respectively, in Refs. (Voronov and Ponomarev (1990)) and (Lv et al. (2021)).

Other topics

There are essentially three current lines of research in the domain of GR physics: (i) use well-established experimental data as a benchmark for new theories; (ii) identify GRs in neutron-rich, eventually weakly-bound isotopes close to the drip lines; (iii) identify elusive modes that have not been seen so far.

Concerning (i), we should mention that, while DFT is a sort of mature theory, still there is much work to be done to improve *ab initio* calculations. *Ab initio* approaches use some technique to solve the many-body problem that is in principle exact, or systematically improvable, and can provide a reliable estimate of the theoretical error of the predicted quantities. Starting from the basic theory of strong interactions, that is Quantum Chromo Dynamics (QCD), there is no unique way to derive a low-energy effective Hamiltonian. This would not be a problem at all, if there were different Hamiltonians that predict compatible values for the different observables. So far, the different Hamiltonians are not accurate enough, and there are discrepancies between the results of different Hamiltonians when used within a given many-body method. In this respect, GR physics is a formidable and unique playground to fix procedures that guarantee that those low-energy effective Hamiltonians capture the most important nuclear correlations.

The multipole response of unstable nuclei, and the possible occurrence of new exotic modes of excitation in weakly-bound nuclear systems, has been the subject of the review paper (Paar et al. (2007)). Many of the theoretical tools that we have described in this chapter were introduced in that review paper, except for the new developments that have taken place after 2007. The evolution of the low-energy dipole response in unstable neutron-rich nuclei is a topic that has been subject of strong interest, and is also subject of another chapter in this Handbook. There exist isotopic chains along which some low-energy or “pygmy” resonances seem to develop; but, often, the available empirical information is not sufficient to determine the nature of these pygmy resonances. Monopole, quadrupole, or spin pygmy states have been proposed in the recent literature.

As we said, one often looks for possible new, elusive modes. This may be simply curiosity-driven, or may be related to specific goals. However, one of the strongest reasons to study GRs is their link with the nuclear Equation of State (EoS). The EoS is the function (not functional here) $E[\rho_n, \rho_p]$ in uniform nuclear matter. The review paper (Roca-Maza and Paar (2018)) summarises the present constraints to the EoS, around the saturation density of symmetric matter, from nuclear structure calculations of ground and collective excited state properties of atomic nuclei. Not only the ISGMR is linked to the nuclear incompressibility, but the dipole response is connected to the so-called symmetry energy and its density dependence. The symmetry energy $S(\rho)$ is the energy per particle to change protons into neutrons, starting from

symmetric matter at a given density. Knowing this sector of the EoS is of paramount importance for our understanding of dilute, neutron-rich systems, or of neutron stars.

Often, a nice correlation shows up between GR properties (energy of the IS-GMR, or of the IVGDR) and some parameter of the EoS. This can be seen in (Garg and Colò (2018)) and in several figures of (Roca-Maza and Paar (2018)) (cf. also the Table 2 in this latter paper, and the references quoted therein). These correlations appear, as a rule, when working at the level of (Q)RPA. As we have discussed, the main effect of coupling to phonons or 2p-2h is a shift downward of the GR peak energy. In some cases, this shift is small enough so that it can be neglected [cf. the monopole case as discussed in (Garg and Colò (2018))]. More often, this shift is of the order of ≈ 1 MeV or slightly more. It does not markedly depend on the chosen effective Hamiltonian or EDF. Unfortunately, it breaks the nice correlation that exists between (Q)RPA results and EoS parameters. Pragmatic approaches, that amount to assuming that the correlation that holds at the (Q)RPA level is simply shifted by the aforementioned quantity of about 1 MeV, could be assumed (Niu et al. (2012), Tselyaev et al. (2016)). Analysing in a deeper manner the link between the GR properties and the EoS beyond (Q)RPA is still an open issue.

References

- D.P. Arteaga, P. Ring, Relativistic random-phase approximation in axial symmetry. *Phys. Rev. C - Nucl. Phys.* **77**(3), 034317 (2008). <https://doi.org/10.1103/PhysRevC.77.034317>. <https://journals-aps-org.pros1.lib.unimi.it/prc/abstract/10.1103/PhysRevC.77.034317>
- P. Avogadro, T. Nakatsukasa, Finite amplitude method for the quasiparticle random-phase approximation. *Phys. Rev. C - Nucl. Phys.* **84**(1), 014314 (2011). <https://doi.org/10.1103/PhysRevC.84.014314>. <https://journals.aps.org/prc/abstract/10.1103/PhysRevC.84.014314>
- V. Baran, M. Colonna, V. Greco, M. Di Toro, *Reaction dynamics with exotic nuclei* (Elsevier, 2005). <https://doi.org/10.1016/j.physrep.2004.12.004>
- M. Bender, P.-H. Heenen, P.-G. Reinhard, Self-consistent mean-field models for nuclear structure (2003). <https://journals-aps-org.pros.lib.unimi.it:2050/rmp/pdf/10.1103/RevModPhys.75.121>
- H. Berghammer, D. Vretenar, P. Ring, Computer program for the time-evolution of a nuclear system in relativistic mean-field theory. *Comput. Phys. Commun.* **88**(2-3), 293–308 (1995). [https://doi.org/10.1016/0010-4655\(95\)00018-B](https://doi.org/10.1016/0010-4655(95)00018-B)
- B.L. Berman, S.C. Fultz, Measurements of the giant dipole resonance with monoenergetic photons. *Rev. Mod. Phys.* **47**(3), 713–761 (1975). <https://doi.org/10.1103/RevModPhys.47.713>. <https://journals-aps-org.pros.lib.unimi.it/rmp/abstract/10.1103/RevModPhys.47.713>
- G.F. Bertsch, P.F. Bortignon, R.A. Broglia, Damping of nuclear excitations. *Rev. Mod. Phys.* **55**(1), 287–314 (1983). <https://doi.org/10.1103/RevModPhys.55.287>. <https://journals-aps-org.pros1.lib.unimi.it/rmp/abstract/10.1103/RevModPhys.55.287>
- A. Bjelčić, T. Nikšić, Implementation of the quasiparticle finite amplitude method within the relativistic self-consistent mean-field framework: The program DIRQFAM. *Comput. Phys. Commun.* **253**, 107184 (2020). <https://doi.org/10.1016/j.cpc.2020.107184>
- J.P. Blaizot, *Nuclear compressibilities* (North-Holland, 1980). [https://doi.org/10.1016/0370-1573\(80\)90001-0](https://doi.org/10.1016/0370-1573(80)90001-0)
- P.F. Bortignon, A. Bracco, R.A. Broglia, *Giant Resonances* (CRC Press, ???, 1998). <https://doi.org/10.1201/9780203753224>

- G.E. Brown, M. Bolsterli, Dipole state in nuclei. *Phys. Rev. Lett.* **3**(10), 472–476 (1959). <https://doi.org/10.1103/PhysRevLett.3.472>. <https://journals-aps-org.pros1.lib.unimi.it/prl/abstract/10.1103/PhysRevLett.3.472>
- S. Burrello, M. Colonna, G. Colò, D. Lacroix, X. Roca-Maza, G. Scamps, H. Zheng, Interplay between low-lying isoscalar and isovector dipole modes: A comparative analysis between semi-classical and quantum approaches (2019). <https://doi.org/10.1103/PhysRevC.99.054314>
- G. Colò, P.F. Bortignon, QRPA plus phonon coupling model and the photoabsorption cross section for 18,20,22O. *Nucl. Phys. A* **696**(3-4), 427–441 (2001). [https://doi.org/10.1016/S0375-9474\(01\)01217-9](https://doi.org/10.1016/S0375-9474(01)01217-9)
- G. Colò, N. Van Giai, P.F. Bortignon, R.A. Broglia, Escape and spreading properties of charge-exchange resonances in Bi208. *Phys. Rev. C* **50**(3), 1496–1508 (1994). <https://doi.org/10.1103/PhysRevC.50.1496>. <https://journals.aps.org/prc/abstract/10.1103/PhysRevC.50.1496>
- G. Colò, D. Gambacurta, W. Kleinig, J. Kvasil, V.O. Nesterenko, A. Pastore, Isoscalar monopole and quadrupole modes in Mo isotopes: Microscopic analysis. *Phys. Lett. Sect. B Nucl. Elem. Part. High-Energy Phys.* **811**, 135940 (2020). <https://doi.org/10.1016/j.physletb.2020.135940>
- V. De Donno, G. Co', M. Anguiano, A.M. Lallena, Self-consistent continuum random-phase approximation calculations with finite-range interactions. *Phys. Rev. C - Nucl. Phys.* **83**(4), 044324 (2011). <https://doi.org/10.1103/PhysRevC.83.044324>. <https://journals-aps-org.pros1.lib.unimi.it/prc/abstract/10.1103/PhysRevC.83.044324>
- V. De Donno, G. Co, M. Anguiano, A.M. Lallena, Self-consistent continuum random-phase approximation with finite-range interactions for charge-exchange excitations. *Phys. Rev. C* **93**(3), 034320 (2016). <https://doi.org/10.1103/PhysRevC.93.034320>. <https://journals-aps-org.pros1.lib.unimi.it/prc/abstract/10.1103/PhysRevC.93.034320>
- J.M. Eisenberg, W. Greiner, *Nuclear Theory. Excitation mechanisms of the nucleus. Vol. 2* (North-Holland, Amsterdam, 1976)
- J. Endres, E. Litvinova, D. Savran, P.A. Butler, M.N. Harakeh, S. Harissopoulos, R.D. Herzberg, R. Krücken, A. Lagoyannis, N. Pietralla, V. Ponomarev, L. Popescu, P. Ring, M. Scheck, K. Sonnabend, V.I. Stoica, H.J. Wörtche, A. Zilges, Isospin character of the pygmy dipole resonance in Sn124. *Phys. Rev. Lett.* **105**(21), 212503 (2010). <https://doi.org/10.1103/PhysRevLett.105.212503>. <https://journals.aps.org/prl/abstract/10.1103/PhysRevLett.105.212503>
- D. Gambacurta, M. Grasso, J. Engel, Subtraction method in the second random-phase approximation: First applications with a Skyrme energy functional. *Phys. Rev. C - Nucl. Phys.* **92**(3), 034303 (2015). <https://doi.org/10.1103/PhysRevC.92.034303>. <https://journals-aps-org.pros1.lib.unimi.it/prc/abstract/10.1103/PhysRevC.92.034303>
- D. Gambacurta, M. Grasso, J. Engel, Gamow-Teller Strength in Ca 48 and Ni 78 with the Charge-Exchange Subtracted Second Random-Phase Approximation. *Phys. Rev. Lett.* **125**(21), 212501 (2020). <https://doi.org/10.1103/PhysRevLett.125.212501>. <https://journals-aps-org.pros1.lib.unimi.it/prl/abstract/10.1103/PhysRevLett.125.212501>
- D. Gambacurta, M. Grasso, V. De Donno, G. Co', F. Catara, Second random-phase approximation with the Gogny force: First applications. *Phys. Rev. C - Nucl. Phys.* **86**(2), 021304 (2012). <https://doi.org/10.1103/PhysRevC.86.021304>. <https://journals-aps-org.pros1.lib.unimi.it/prc/abstract/10.1103/PhysRevC.86.021304>
- U. Garg, G. Colò, *The compression-mode giant resonances and nuclear incompressibility* (Elsevier B.V., 2018). <https://doi.org/10.1016/j.ppnp.2018.03.001>
- P.M. Goddard, N. Cooper, V. Werner, G. Rusev, P.D. Stevenson, A. Rios, C. Bernards, A. Chakraborty, B.P. Crider, J. Glorius, R.S. Ilieva, J.H. Kelley, E. Kwan, E.E. Peters, N. Pietralla, R. Raut, C. Romig, D. Savran, L. Schnorrenberger, M.K. Smith, K. Sonnabend, A.P. Tonchev, W. Tornow, S.W. Yates, Dipole response of 76Se above 4 MeV. *Phys. Rev. C - Nucl. Phys.* **88**(6), 064308 (2013). <https://doi.org/10.1103/PhysRevC.88.064308>. <https://journals-aps-org.pros1.lib.unimi.it/prc/abstract/10.1103/PhysRevC.88.064308>
- M.L. Gorelik, S. Shlomo, B.A. Tulupov, M.H. Urin, Properties of isoscalar giant multipole resonances in medium-heavy closed-shell nuclei: A semimicroscopic descrip-

- tion. Phys. Rev. C **103**(3), 034302 (2021). <https://doi.org/10.1103/PhysRevC.103.034302>.
<https://journals.aps.org/prc/abstract/10.1103/PhysRevC.103.034302>
- S. Goriely, S. Hilaire, M. Girod, S. Péru, First Gogny-Hartree-Fock-Bogoliubov nuclear mass model. Phys. Rev. Lett. **102**(24), 242501 (2009). <https://doi.org/10.1103/PhysRevLett.102.242501>. <https://journals-aps-org.pros1.lib.unimi.it/prl/abstract/10.1103/PhysRevLett.102.242501>
- I. Hamamoto, H. Sagawa, X.Z. Zhang, Giant monopole resonances in nuclei near stable and drip lines. Phys. Rev. C - Nucl. Phys. **56**(6), 3121–3133 (1997a). <https://doi.org/10.1103/PhysRevC.56.3121>. <https://journals.aps.org/prc/abstract/10.1103/PhysRevC.56.3121>
- I. Hamamoto, H. Sagawa, X.Z. Zhang, Structure of giant quadrupole resonances in neutron drip line nuclei. Phys. Rev. C - Nucl. Phys. **55**(5), 2361–2365 (1997b). <https://doi.org/10.1103/PhysRevC.55.2361>. <https://journals-aps-org.pros1.lib.unimi.it/prc/abstract/10.1103/PhysRevC.55.2361>
- I. Hamamoto, H. Sagawa, X.Z. Zhang, Isoscalar and isovector dipole mode in drip line nuclei in comparison with β -stable nuclei. Phys. Rev. C - Nucl. Phys. **57**(3), 1064 (1998). <https://doi.org/10.1103/physrevc.57.r1064>. <https://journals.aps.org/prc/abstract/10.1103/PhysRevC.57.R1064>
- M.N. Harakeh, A. van der Woude, *Giant resonances: Fundamental high frequency modes of nuclear excitation* (Clarendon Press, ???, 2001). ISBN 0198517335. <https://research.rug.nl/en/publications/giant-resonances-fundamental-high-frequency-modes-of-nuclear-exci>
- S. Kamerdzhev, J. Speth, G. Tertychny, *Extended theory of finite Fermi systems: Collective vibrations in closed shell nuclei* (North-Holland, 2004). <https://doi.org/10.1016/j.physrep.2003.11.001>
- E. Khan, N. Sandulescu, M. Grasso, N. Van Giai, Continuum quasiparticle random phase approximation and the time-dependent Hartree-Fock-Bogoliubov approach. Phys. Rev. C - Nucl. Phys. **66**(2), 243091–243099 (2002). <https://doi.org/10.1103/PhysRevC.66.024309>. <https://journals-aps-org.pros2.lib.unimi.it/prc/abstract/10.1103/PhysRevC.66.024309>
- M. Kortelainen, N. Hinohara, W. Nazarewicz, Multipole modes in deformed nuclei within the finite amplitude method. Phys. Rev. C - Nucl. Phys. **92**(5), 051302 (2015). <https://doi.org/10.1103/PhysRevC.92.051302>. <https://journals.aps.org/prc/abstract/10.1103/PhysRevC.92.051302>
- G.A. Lalazissis, T. Nikšić, D. Vretenar, P. Ring, New relativistic mean-field interaction with density-dependent meson-nucleon couplings. Phys. Rev. C - Nucl. Phys. **71**(2), 024312 (2005). <https://doi.org/10.1103/PhysRevC.71.024312>. <https://journals-aps-org.pros1.lib.unimi.it/prc/abstract/10.1103/PhysRevC.71.024312>
- E. Litvinova, P. Ring, V. Tselyaev, Particle-vibration coupling within covariant density functional theory. Phys. Rev. C - Nucl. Phys. **75**(6), 064308 (2007). <https://doi.org/10.1103/PhysRevC.75.064308>. <https://journals-aps-org.pros1.lib.unimi.it/prc/abstract/10.1103/PhysRevC.75.064308>
- E. Litvinova, P. Ring, V. Tselyaev, Relativistic quasiparticle time blocking approximation: Dipole response of open-shell nuclei. Phys. Rev. C - Nucl. Phys. **78**(1), 014312 (2008). <https://doi.org/10.1103/PhysRevC.78.014312>. <https://journals-aps-org.pros1.lib.unimi.it/prc/abstract/10.1103/PhysRevC.78.014312>
- E. Litvinova, P. Schuck, Toward an accurate strongly coupled many-body theory within the equation-of-motion framework. Phys. Rev. C **100**(6), 064320 (2019a). <https://doi.org/10.1103/PhysRevC.100.064320>. <https://journals.aps.org/prc/abstract/10.1103/PhysRevC.100.064320>
- E. Litvinova, P. Schuck, Toward an accurate strongly coupled many-body theory within the equation-of-motion framework. Phys. Rev. C **100**(6), 064320 (2019b). <https://doi.org/10.1103/PhysRevC.100.064320>. <https://journals.aps.org/prc/abstract/10.1103/PhysRevC.100.064320>

- E. Litvinova, P. Schuck, Many-body correlations in nuclear superfluidity. *Phys. Rev. C* **102**(3), 034310 (2020). <https://doi.org/10.1103/PhysRevC.102.034310>. <https://journals.aps.org/prc/abstract/10.1103/PhysRevC.102.034310>
- W.L. Lv, Y.F. Niu, G. Colò, Learning about the structure of giant resonances from their γ decay. *Phys. Rev. C* **103**(6), 064321 (2021). <https://doi.org/10.1103/PhysRevC.103.064321>. <https://journals.aps.org/prc/abstract/10.1103/PhysRevC.103.064321>
- J.A. Maruhn, P.G. Reinhard, P.D. Stevenson, A.S. Umar, The TDHF code Sky3D. *Comput. Phys. Commun.* **185**(7), 2195–2216 (2014). <https://doi.org/10.1016/j.cpc.2014.04.008>
- T. Nakatsukasa, T. Inakura, K. Yabana, Finite amplitude method for the solution of the random-phase approximation. *Phys. Rev. C - Nucl. Phys.* **76**(2), 024318 (2007). <https://doi.org/10.1103/PhysRevC.76.024318>. <https://journals.aps.org/prc/abstract/10.1103/PhysRevC.76.024318>
- T. Nakatsukasa, K. Matsuyanagi, M. Matsuo, K. Yabana, Time-dependent density-functional description of nuclear dynamics. *Rev. Mod. Phys.* **88**(4) (2016). <https://doi.org/10.1103/RevModPhys.88.045004>. <https://journals-aps-org.pros.lib.unimi.it:2050/rmp/pdf/10.1103/RevModPhys.88.045004>
- Y.F. Niu, G. Colò, E. Vigezzi, Gamow-Teller response and its spreading mechanism in doubly magic nuclei. *Phys. Rev. C - Nucl. Phys.* **90**(5), 054328 (2014). <https://doi.org/10.1103/PhysRevC.90.054328>. <https://journals.aps.org/prc/abstract/10.1103/PhysRevC.90.054328>
- Y.F. Niu, G. Colò, M. Brenna, P.F. Bortignon, J. Meng, Gamow-Teller response within Skyrme random-phase approximation plus particle-vibration coupling. *Phys. Rev. C - Nucl. Phys.* **85**(3), 034314 (2012). <https://doi.org/10.1103/PhysRevC.85.034314>. <https://journals-aps-org.pros2.lib.unimi.it/prc/abstract/10.1103/PhysRevC.85.034314>
- Y.F. Niu, G. Colò, E. Vigezzi, C.L. Bai, H. Sagawa, Quasiparticle random-phase approximation with quasiparticle-vibration coupling: Application to the Gamow-Teller response of the superfluid nucleus Sn 120. *Phys. Rev. C* **94**(6), 064328 (2016). <https://doi.org/10.1103/PhysRevC.94.064328>. <https://journals.aps.org/prc/abstract/10.1103/PhysRevC.94.064328>
- N. Paar, D. Vretenar, E. Khan, G. Colò, Exotic modes of excitation in atomic nuclei far from stability. *Reports Prog. Phys.* **70**(5) (2007). <https://doi.org/10.1088/0034-4885/70/5/R02>
- P. Papakonstantinou, Second random-phase approximation, Thouless' theorem, and the stability condition reexamined and clarified. *Phys. Rev. C - Nucl. Phys.* **90**(2), 024305 (2014). <https://doi.org/10.1103/PhysRevC.90.024305>. <https://journals-aps-org.pros2.lib.unimi.it/prc/abstract/10.1103/PhysRevC.90.024305>
- P. Papakonstantinou, R. Roth, Large-scale second random-phase approximation calculations with finite-range interactions. *Phys. Rev. C - Nucl. Phys.* **81**(2), 024317 (2010). <https://doi.org/10.1103/PhysRevC.81.024317>. <https://journals-aps-org.pros2.lib.unimi.it/prc/abstract/10.1103/PhysRevC.81.024317>
- V.Y. Ponomarev, P.F. Bortignon, R.A. Broglia, V.V. Voronov, Damping width of double resonances. *Zeitschrift für Phys. A Hadron. Nucl.* **356**(1), 251–254 (1996). <https://doi.org/10.1007/bf02769226>. <https://link.springer.com/article/10.1007/BF02769226>
- V.Y. Ponomarev, P.F. Bortignon, R.A. Broglia, V.V. Voronov, Anharmonic properties of the double giant dipole resonance. *Phys. Rev. Lett.* **85**(7), 1400–1403 (2000). <https://doi.org/10.1103/PhysRevLett.85.1400>. <https://journals.aps.org/prl/abstract/10.1103/PhysRevLett.85.1400>
- V.Y. Ponomarev, P.F. Bortignon, R.A. Broglia, V.V. Voronov, Microscopic studies of multiphonon resonances. *Nucl. Phys. A* **687**(1-2), 170–177 (2001). [https://doi.org/10.1016/S0375-9474\(01\)00617-0](https://doi.org/10.1016/S0375-9474(01)00617-0)
- P. Ring, P. Schuck, *The Nuclear Many-Body Problem* (Springer Berlin Heidelberg, ???, 1980). <https://doi.org/10.1007/978-3-642-61852-9>
- C. Robin, E. Litvinova, Time-Reversed Particle-Vibration Loops and Nuclear Gamow-Teller Response. *Phys. Rev. Lett.* **123**(20),

- 202501 (2019). <https://doi.org/10.1103/PhysRevLett.123.202501>.
<https://journals.aps.org/prl/abstract/10.1103/PhysRevLett.123.202501>
- X. Roca-Maza, N. Paar, *Nuclear equation of state from ground and collective excited state properties of nuclei* (Elsevier B.V., 2018). <https://doi.org/10.1016/j.ppnp.2018.04.001>
- X. Roca-Maza, G. Colò, H. Sagawa, New Skyrme interaction with improved spin-isospin properties. *Phys. Rev. C - Nucl. Phys.* **86**(3), 031306 (2012). <https://doi.org/10.1103/PhysRevC.86.031306>. <https://journals-aps-org.pros1.lib.unimi.it/prc/abstract/10.1103/PhysRevC.86.031306>
- X. Roca-Maza, Y.F. Niu, G. Colo, P.F. Bortignon, Towards a self-consistent dynamical nuclear model. *J. Phys. G Nucl. Part. Phys.* **44**(4), 21 (2017). <https://doi.org/10.1088/1361-6471/aa5669>
- D.J. Rowe, *Nuclear collective motion: Models and theory* (Methuen, ???, 1970), pp. 1–342. ISBN 9789812790668. <https://doi.org/10.1142/6721>
- D. Savran, M. Fritzsche, J. Hasper, K. Lindenberg, S. Müller, V.Y. Ponomarev, K. Sonnabend, A. Zilges, Fine structure of the pygmy dipole resonance in Xe136. *Phys. Rev. Lett.* **100**(23), 232501 (2008). <https://doi.org/10.1103/PhysRevLett.100.232501>. <https://journals.aps.org/prl/abstract/10.1103/PhysRevLett.100.232501>
- G. Scamps, D. Lacroix, Systematic study of isovector and isoscalar giant quadrupole resonances in normal and superfluid deformed nuclei. *Phys. Rev. C - Nucl. Phys.* **89**(3), 034314 (2014). <https://doi.org/10.1103/PhysRevC.89.034314>. <https://journals-aps-org.pros2.lib.unimi.it/prc/abstract/10.1103/PhysRevC.89.034314>
- B. Schuetrumpf, P.-G. Reinhard, P.D. Stevenson, A.S. Umar, J.A. Maruhn, The TDHF Code Sky3D Version 1.1 Title: The TDHF Code Sky3D Version 1.1, Technical report, 2018. <http://www.elsevier.com/open-access/userlicense/1.0/>
- S. Shen, G. Colò, X. Roca-Maza, Particle-vibration coupling for giant resonances beyond the diagonal approximation. *Phys. Rev. C* **101**(4), 044316 (2020). <https://doi.org/10.1103/PhysRevC.101.044316>. <https://journals.aps.org/prc/abstract/10.1103/PhysRevC.101.044316>
- A. Shevchenko, J. Carter, R.W. Fearick, S.V. Förtisch, H. Fujita, Y. Fujita, Y. Kalmykov, D. Lacroix, J.J. Lawrie, P. Von Neumann-Cosel, R. Neveling, V.Y. Ponomarev, A. Richter, E. Sideras-Haddad, F.D. Smit, J. Wambach, Fine structure in the energy region of the isoscalar giant quadrupole resonance: Characteristic scales from a wavelet analysis. *Phys. Rev. Lett.* **93**(12), 122501 (2004). <https://doi.org/10.1103/PhysRevLett.93.122501>. <https://journals.aps.org/prl/abstract/10.1103/PhysRevLett.93.122501>
- V.G. Soloviev, *Theory of Atomic Nuclei, Quasi-particle and Phonons* (CRC Press, ???, 1992)
- J. Suhonen, *From Nucleons to Nucleus. Theoretical and Mathematical Physics* (Springer, Berlin, Heidelberg, 2007). ISBN 978-3-540-48859-0. <https://doi.org/10.1007/978-3-540-48861-3>. <http://link.springer.com/10.1007/978-3-540-48861-3>
- V.I. Tselyaev, Subtraction method and stability condition in extended random-phase approximation theories. *Phys. Rev. C - Nucl. Phys.* **88**(5), 054301 (2013). <https://doi.org/10.1103/PhysRevC.88.054301>. <https://journals-aps-org.pros1.lib.unimi.it/prc/abstract/10.1103/PhysRevC.88.054301>
- V. Tselyaev, N. Lyutorovich, J. Speth, S. Krewald, P.G. Reinhard, Application of an extended random-phase approximation to giant resonances in light-, medium-, and heavy-mass nuclei. *Phys. Rev. C* **94**(3), 034306 (2016). <https://doi.org/10.1103/PhysRevC.94.034306>. <https://journals-aps-org.pros1.lib.unimi.it/prc/abstract/10.1103/PhysRevC.94.034306>
- N. Van Giai, H. Sagawa, Monopole and dipole compression modes in nuclei. *Nucl. Physics, Sect. A* **371**(1), 1–18 (1981). [https://doi.org/10.1016/0375-9474\(81\)90741-7](https://doi.org/10.1016/0375-9474(81)90741-7)
- V. Voronov, V. Ponomarev, Gamma - decay of giant resonances. *Nucl. Physics, Sect. A* **520**(C), 619–626 (1990). [https://doi.org/10.1016/0375-9474\(90\)91179-U](https://doi.org/10.1016/0375-9474(90)91179-U)
- D. Vretenar, A.V. Afanasjev, G.A. Lalazissis, P. Ring, Relativistic Hartree-Bogoliubov theory: static and dynamic aspects of exotic nuclear structure. *Phys. Rep.* **409**, 101–259 (2005). <https://doi.org/10.1016/j.physrep.2004.10.001>. www.elsevier.com/locate/physrep

- C. Yannouleas, Zero-temperature second random phase approximation and its formal properties. *Phys. Rev. C* **35**(3), 1159–1161 (1987). <https://doi.org/10.1103/PhysRevC.35.1159>. <https://journals-aps-org.pros1.lib.unimi.it/prc/abstract/10.1103/PhysRevC.35.1159>
- J. Yasuda, M. Sasano, R.G.T. Zegers, H. Baba, D. Bazin, W. Chao, M. Dozono, N. Fukuda, N. Inabe, T. Isobe, G. Jhang, D. Kameda, M. Kaneko, K. Kisamori, M. Kobayashi, N. Kobayashi, T. Kobayashi, S. Koyama, Y. Kondo, A.J. Krasznahorkay, T. Kubo, Y. Kubota, M. Kurata-Nishimura, C.S. Lee, J.W. Lee, Y. Matsuda, E. Milman, S. Michimasa, T. Motobayashi, D. Muecher, T. Murakami, T. Nakamura, N. Nakatsuka, S. Ota, H. Otsu, V. Panin, W. Powell, S. Reichert, S. Sakaguchi, H. Sakai, M. Sako, H. Sato, Y. Shimizu, M. Shikata, S. Shimoura, L. Stuhl, T. Sumikama, H. Suzuki, S. Tangwanchaoen, M. Takaki, H. Takeda, T. Tako, Y. Togano, H. Tokieda, J. Tsubota, T. Uesaka, T. Wakasa, K. Yako, K. Yoneda, J. Zenihiro, Extraction of the Landau-Migdal Parameter from the Gamow-Teller Giant Resonance in Sn 132. *Phys. Rev. Lett.* **121**(13), 132501 (2018). <https://doi.org/10.1103/PhysRevLett.121.132501>. <https://journals.aps.org/prl/abstract/10.1103/PhysRevLett.121.132501>
- K. Yoshida, Isovector giant monopole and quadrupole resonances in a Skyrme energy density functional approach with axial symmetry. *Phys. Rev. C* **104**(4), 044309 (2021). <https://doi.org/10.1103/PhysRevC.104.044309>. <https://journals.aps.org/prc/abstract/10.1103/PhysRevC.104.044309>